Generation of Novel Copper Sites by Mutation of the Axial Ligand of Amicyanin. Atomic Resolution Structures and Spectroscopic Properties[†,‡]

Christopher J. Carrell,[§] John K. Ma,[∥] William E. Antholine,[⊥] Jonathan P. Hosler,[∥] F. Scott Mathews,*[,§] and Victor L. Davidson*[,∥]

Department of Biochemistry and Molecular Biophysics, Washington University School of Medicine, St. Louis, Missouri 63110, Department of Biochemistry, The University of Mississippi Medical Center, Jackson, Mississippi 39216-4505, and Department of Biophysics, Medical College of Wisconsin, Milwaukee, Wisconsin 53226

Received September 21, 2006; Revised Manuscript Received November 27, 2006

ABSTRACT: Amicyanin from *Paracoccus denitrificans* is a type 1 copper protein with three strong equatorial copper ligands provided by nitrogens of His53 and His95 and the sulfur of Cys92, with an additional weak axial ligand provided by the sulfur of Met98. Met98 was replaced with either Gln or Ala. As isolated, the M98A and M98Q mutant proteins contain zinc in the active site. The zinc is then removed and replaced with copper so that the copper-containing proteins may be studied. Each of the mutant amicyanins exhibits a marked decrease in thermal stability relative to that of native amicyanin, consistent with the weaker affinity for copper. Crystal structures were obtained for the oxidized and reduced forms of M98A and M98Q amicyanins at atomic resolution (≤1.0 Å). The crystal structure of oxidized M98A amicyanin exhibits a type 1 ligation geometry but with the axial ligand provided by a water, which fills the void left by the mutation of Met to Ala. The protein undergoes a reversible switch in ligation geometry when going from the aqueous to the frozen state. The visible absorption spectrum in solution is characteristic of type 1 copper, consistent with the crystal structure. On freezing, the blue color is lost, and EPR spectroscopy reveals that the copper is primarily type 2. The crystal structure of reduced M98A amicyanin exhibits an unprecedented ligation geometry in which the His95−Cu coordination is broken, and copper is left with only two ligands from His53 and Cys92 in an almost linear coordination. The replacement of Met98 with Gln yielded a type 1 copper site with increased rhombicity evident from its EPR and visible absorption spectra, and an increase in distance from Cu to the trigonal equatorial plane seen in the crystal structure. Gln98 coordinates more strongly with copper than Met, and the oxidized and reduced forms each exhibit two alternate conformers. EPR and metal analysis of oxidized M98Q amicyanin indicate that a small population of the protein contains weakly bound type 2 copper, which may be removed by washing with EDTA. These results demonstrate that the identity as well as position and rigidity of the axial ligand of the type 1 copper site has a profound influence in the uptake specificity of metal ions, protein stability, and determination of the active site geometry and its spectroscopic properties.

Copper proteins are abundant in nature and exhibit a wide range of catalytic and electron-transfer functions. The protein-bound copper centers are classified according to their spectroscopic properties as type 1, type 2, or type 3. Type 1 (also called blue) copper proteins exhibit an intense blue color relative to that of inorganic copper complexes and unusually small hyperfine coupling constants in the EPR spectrum of the oxidized protein. Type 1 copper sites are found in a wide range of electron-transfer proteins, including amicyanin and azurin in bacteria and plastocyanin in plants, and in multicopper proteins, such as ascorbate oxidase and ceruloplasmin, which are found in animals as well (*1*). The active site of type 1 cupredoxins typically consists of three strong equatorial ligands, two N of two His and S of a Cys, forming a trigonal plane plus an additional axial ligand, usually provided by a Met (*1*). Azurin is unusual in that two axial ligands are present, S provided by a Met and an O provided by the backbone carbonyl of a Gly, giving that copper site a 5-coordinate, trigonal bipyramidal geometry (*2*).

Among the blue copper proteins, exceptions to the presence of Met as the axial fourth ligand do occur and

[†] This work was supported by NSF Grant MCB0343374 (to F.S.M.) and NIH Grants GM-41574 (to V.L.D.), EB001980 (to W.E.A. Co-P.I.), and GM-56824 (to J.P.H.). The use of the Advanced Photon Source was supported by the U.S. Department of Energy, Office of Science, Office of Basic Energy Sciences, under Contract No. W-31-109-ENG-38.

[‡] Crystallographic coordinates have been deposited in the Protein Data Bank under file names 2IDQ (M98A Cu(II)), 2IDS (M98A Cu(I)), 2IDT (M98Q Cu(II)), and 2IDU (M98Q Cu(I)).

* Corresponding author. Tel: 314-362-1080. Fax: 314-362-7183. E-mail: mathews@biochem.wustl.edu (F.S.M.). Tel: 601-984-1516. Fax: 601-984-1501. E-mail: vdavidson@biochem.umsmed.edu (V.L.D.).

[§] Washington University School of Medicine.

[∥] The University of Mississippi Medical Center.

[⊥] Medical College of Wisconsin.

[1] Abbreviations: MADH, methylamine dehydrogenase; TTQ, tryptophan tryptophylquinone; EDTA, ethylenediaminetetraacetic acid; DTT, dithiothreitol; ICP-OES, inductively coupled plasma optical emission spectroscopy; DSC, differential scanning calorimetry; rmsd, root mean square difference; EPR, electron paramagnetic resonance.

10.1021/bi0619674 CCC: $37.00
Published on Web 01/18/2007

include phytocyanins such as stellacyanin, which possesses a glutamine in this position (*3*), and the multicopper proteins laccase (*4*) and ceruloplasmin (*5*), which possess a leucine in this position in their type 1 centers. Depending on the nature and presence of an axial fourth ligand, the extent to which the copper is out of the equatorial plane varies. Structural and spectroscopic characterization of the copper site in relationship to the equatorial plane have classified type 1 copper sites into axial and rhombic forms. In the axial form, exemplified by amicyanin (*6*), azurin (*7*), and plastocyanin (*8*), a strongly in-plane trigonal copper coordination predominates with a long, weak bond to the axial ligand. In the rhombic form, exemplified by stellacyanin and phytocyanins (*9*), the copper ion is pulled away from the equatorial plane by a strong axial ligand (*10*).

In this article, site-directed mutagenesis was used to alter the axial ligand of amicyanin and determine the precise contributions of the identity and position of the axial ligand in dictating the structure and spectroscopic properties of type 1 copper proteins. Amicyanin is the central component of one of the best characterized physiologic electron-transfer complexes of proteins that is formed by methylamine dehydrogenase (MADH) (*11*), amicyanin (*12*), and cytochrome *c*-551i (*13*) from *Paracoccus denitrificans*. X-ray crystal structures are available for the binary complex of MADH and amicyanin (*14*) and for a ternary protein complex, which includes cytochrome *c*-551i, the electron acceptor for amicyanin (*15*). Site-directed mutagenesis of amicyanin has been performed previously to elucidate the roles of specific amino acid residues in determining its redox and electron-transfer properties (*16*−*20*). In *P. denitrificans* amicyanin, Met98 provides the axial S ligand with the three equatorial ligands provided by His53, Cys92, and His95 (*6*). In the present study, Met98 of amicyanin is changed to Gln and Ala via site-directed mutagenesis to determine the influence of the axial ligand on the structure and spectroscopic properties of type 1 copper proteins.

Crystal structures were obtained for the oxidized and reduced forms of M98A and M98Q amicyanins at atomic resolution. Effects of these mutations on the metal selectivity of the metal-binding site and stability of the protein are documented. Novel spectroscopic properties of each mutant are described and correlated with the new structures. The results provide new insight into the roles of the axial ligand of the type 1 copper site with regard to the uptake specificity of metal binding during assembly and protein stability, and the factors that dictate active site ligation geometry.

EXPERIMENTAL PROCEDURES

Protein Expression and Isolation. Wild-type amicyanin was purified from *P. denitrificans* as previously described, and protein concentrations were calculated from known extinction coefficients for oxidized amicyanin ($\epsilon_{595} = 4610$ cm^{-1} M^{-1}) (*12*). Site-directed mutagenesis to create M98A and M98Q amicyanins was performed on double stranded pMEG (*21*), which contains *mau*C (*22*), which encodes amicyanin, using forward and reverse mutagenic primers with the Quickchange Site-directed Mutagenesis Kit (Strategene). For M98A amicyanin, the oligonucleotide sequences used to construct the site-directed mutant were 5′-GACTATCACTGTACCCCGCATCCCTTCCAGCGCGGCAAGGTCG-3′ and its complementary DNA. For M98Q amicyanin, the oligonucleotide sequences used to construct the site-directed mutant were 5′-GACTATCACTGTACCCCGCATCCCTTCGCGCGCGGCAAGGTCG-3′ and its complementary DNA. The underlined bases are those that are changed to create the desired mutation. The entire 555-base *mau*C-containing fragment was sequenced to ensure that no second site mutations were present, and none were found. M98A and M98Q amicyanins were expressed in *E. coli* and initially isolated from the periplasmic fraction described for other recombinant amicyanin mutants (*21*).

Protein Reconstitution. As will be discussed later, the majority of the as-isolated M98A and M98Q amicyanins contained zinc rather than copper in the active site. A method of reconstitution (*23*) is required to unfold the protein, remove any metal ions, refold the protein, and incorporate Cu^{2+}. M98A and M98Q amicyanins were incubated in 10 mM HEPES buffer at pH 8.0, containing 6 M guandinine-HCl, 50 mM EDTA, and 2 mM dithiothreitol (DTT). The unfolded apoproteins were then diluted 50-fold into 10 mM HEPES buffer at pH 8.0 containing 5 mM DTT. The proteins were then dialyzed against 100 mM ammonium acetate at pH 8.0, at 4 °C for 4 h, followed by overnight dialysis against 250 mM ammonium acetate at pH 8.0. The dialyzed protein solution was then brought to room temperature and titrated with copper sulfate while monitoring the increase in absorbance at 595 nm. Any excess copper sulfate was removed by buffer exchange and ultrafiltration with a 10 kDa cutoff membrane. For the preparation of the ^{63}Cu-containing M98A and M98Q amicyanins, the aforementioned dialyzed protein solution was brought to room temperature and titrated, while monitoring the increase in absorbance at 595 nm, with ^{63}Cu oxide that had been dissolved in HCl and brought to pH 3.0. Any excess copper sulfate or ^{63}Cu oxide was removed by buffer exchange and ultrafiltration using a 10 kDa cutoff membrane.

X-ray Structure Determination. Structures of the copper-containing reconstituted M98A and M98Q amicyanins were determined. The crystals of M98A and M98Q amicyanins were grown by macroseeding using a 9-to-1 mixture of monobasic sodium (3 M) and dibasic potassium (3 M) phosphate solutions as precipitants, as described previously for amicyanin (*24*). The crystals of each mutant protein are monoclinic, space group $P2_1$, containing one molecule per asymmetric unit and are isomorphous with crystals of the wild-type protein. The cell dimensions are given in Table 1. X-ray diffraction data from crystals of oxidized and reduced M98A amicyanin and reduced M98Q amicyanin were recorded at the Biocars beamline14BM-C of the Advanced Photon Source (APS) with an ADSC-Q4 CCD detector. Data from reduced M98Q amicyanin crystals were recorded at the NE-CAT beamline 8-BM of the APS using an ADSC-Q315 CCD detector. In all cases, the data were recorded at 100 K, using paratone oil (Hampton Research, Laguna Hills, CA) as a cryoprotectant. In each case, two data collection passes were made, one rapid with a 0.5° step size per frame to limit detector saturation by strong reflections and the other, slow with a 0.25° step size to record weaker reflections at a higher signal-to-noise ratio. The maximum resolution for the data recorded from the four crystals ranged from 0.9 to 1.0 Å (Table 1). Data from the reduced forms of the M98A and M98Q amicyanins were recorded from crystals that had been

Table 1: Data Collection and Refinement Statistics

samples	oxidized M98A	reduced M98A	oxidized M98Q	reduced M98Q
		data collection		
wavelength (Å)	0.90000	0.90000	0.9794	0.90000
space group	$P2_1$	$P2_1$	$P2_1$	$P2_1$
a (Å)	28.57	28.21	28.41	28.56
b (Å)	56.10	55.10	55.48	55.40
c (Å)	26.97	26.90	27.04	27.09
β (°)	96.63	95.14	95.17	96.13
beamline	APS BM-14-C	APS BM-14-C	APS BM-8-C	APS BM-14-C
resolution limits (outer shell) (Å)	50−0.90 (0.91−0.90)	50−1.0 (1.02−1.00)	50−1.0 (1.02−1.00)	40−0.95 (0.91−0.90)
# of observations	349433	170339	131528	181720
# unique	52731	41110	35092	47487
*R*merge[a] (outer shell)	0.086 (0.279)	0.069 (0.297)	0.067 (0.093)	0.048 (0.082)
$I/\sigma(I)$[b] (outer shell)	21.1 (2.7)	16.0 (2.7)	31.1 (7.8)	18.4 (10.0)
completeness (outer shell)	84.3% (37.5%)	92.9% (74.3%)	77.7% (38.0%)	90.0% (37.3%)
redundancy	6.6	4.1	3.7	3.8
refinenent				
resolution (Å)	26.79−0.90	28.2−1.0	25.2−1.0	18.6−0.95
$\|F\|/\sigma(\|F\|)$	>0	>0	>0	>0
R_{work}/R_{free}[c]	0.108/0.130	0.125/0.164	0.124/0.158	0.129/0.162
reflections (working/test)	50058/2630	38987/2051	33422/1761	45108/2373
protein atoms	813	820	815	816
solvent/other atoms	201	133	175	123
⟨B⟩ protein[d]	9.0	15.6	11.0	12.4
⟨B⟩ solvent[d]	22.9	28.9	25.9	23.3
rms ΔB (m/m)[4,5] (Å^2)	1.54	2.17	1.60	1.89
rms ΔB (m/s)[d,e] (Å^2)	2.69	3.35	2.62	3.26
rms ΔB (s/s)[d,e] (Å^2)	4.76	5.36	4.05	4.58

[a] $R_{merge} = \Sigma_h\Sigma_i |I(h) - I_i(h)|/\Sigma_h\Sigma_i I_i(h)$, where $I_i(h)$ is the *i*th measurement, and $I(h)$ is the mean measurement of reflection *h*. [b] $I/\sigma(I)$ is the average signal-to-noise ratio for merged reflection intensities. [c] $R = \Sigma_h |F_o - F_c|/\Sigma_h |F_o|$, where F_o and F_c are the observed and calculated structure factor amplitudes, respectively, of reflection *h*. R_{free} is *R* for the test reflection data set (5% of the observed reflections) for cross-validation of the refinement (*37*), R_{work} is *R* for the working reflection set. [d] The *B*-values shown refer to the isotropic equivalent of the anisotropic thermal parameters used during the refinement. [e] Root-mean-square difference in the *B*-factor for bonded atoms; m/m, m/c, and c/c represent main chain−main chain, main chain−side chain, and side chain−side chain bonds, respectively.

incubated for ∼30 min with 10 mM sodium ascorbate in 4 M sodium/potassium phosphate buffer in the ratio 4:1 (pH ∼5.5). All four data sets were processed using DENZO and SCALEPACK (*25*). The data collection statistics are presented in Table 1.

The structures of the oxidized and reduced forms of M98A and M98Q amicyanins were refined directly from the oxidized wild-type protein structures, after the removal of solvent molecules and alternate amino acid conformations using SHELX (*26*). No restraints were placed on the copper−ligand distances. Alternating cycles of refinement and model building in XtalView (*27*) were carried out. Hydrogen atoms, positioned as a riding model, were included in the refinements in SHELX. The temperature factors of all non-hydrogen atoms were refined anisotropically. The refinement statistics can be found in Table 1.

Metal Analysis. Metal contents were determined by inductively coupled plasma optical emission spectroscopy (ICP-OES) using a Spectro Genesis spectrometer. Protein samples of native and mutant amicyanins (4−10 μM) were washed and dialyzed in low metal 20 mM Tris-HCl at pH 7.4 (Fluka) prior to analysis. To determine whether metals were tightly bound, protein samples were incubated in buffer containing 1.0 mM EDTA for 15 min, and then EDTA and any low molecular weight species were removed by buffer exchange and ultrafiltration with a 10 kDa cutoff membrane. Metal contents are reported as per amicyanin molecule on the basis of sulfur content, which is predicted from the amino acid sequence and also determined by ICP-OES of the same samples.

Differential Scanning Calorimetry. Solution DSC was performed, and data was analyzed as described previously for native amicyanin (*28*) with a Calorimetry Sciences Corporation 6100 Nano II DSC with tantalum cells with a nominal volume of 0.33 mL. The buffer and the sample were scanned from 15 to 105 °C. As was reported for native amicyanin, it was not possible to obtain ΔH values for the calorimetric enthalpy of unfolding because of the irreversibility of the thermal denaturation, but it was possible to accurately determine T_m values, which define the midpoint temperature for the thermal transition.

Electron Paramagnetic Resonance Spectroscopy. For multifrequency EPR, three spectrometers were employed. Between 3 and 35 GHz, Varian E109 and E-9 systems operating at 9 GHz (X-band) and 35 GHz (Q-band), respectively, and a low-frequency 3.3 GHz (S-band) system

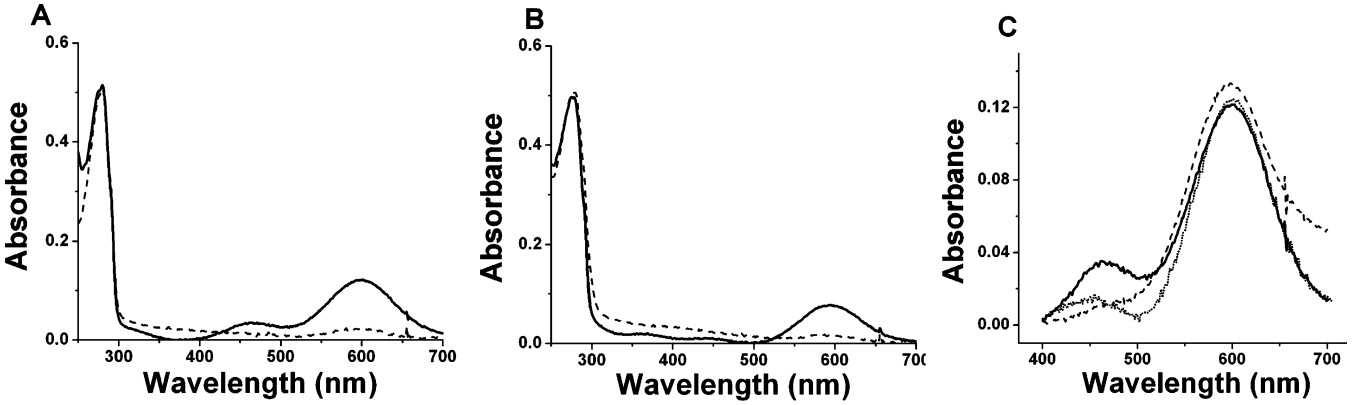

FIGURE 1: Visible absorption spectra of (A) M98Q amicyanin as-isolated (---) and after reconstitution (—) and (B) M98A amicyanin as-isolated (---) and after reconstitution (—). (C) Overlay of the visible absorption of oxidized native (---), M98Q (—) and M98A (···) amicyanins.

based on the loop−gap resonator designed by Froncisz and Hyde (*29*) at the National Biomedical ESR Center, Medical College of Wisconsin, were used. The Q-band bridge was modified with the addition of a GaAs field-effect transistor signal amplifier and low-noise Gunn diode oscillator (*30*). At Q-band, the parameters were as follows: microwave frequency, 35.1 GHz; power, 0.2 mW; modulation amplitude, 5 G; temperature, 50 K; and usually 10 scans averaged. The X-band spectra were collected using a Varian E-9 ESR spectrometer with the following instrumental parameters: microwave frequency, 9.2 GHz; power, 5 mW; modulation amplitude, 5 G; temperature, 133 K; and usually 4 scans averaged. The S-band system consists of a Varian E-9 ESR spectrometer fitted with a low-frequency microwave bridge operating at 3.3 GHz (S-band). The instrument parameters for the S-band spectra were as follows: microwave frequency, 3.33 GHz; power, 0.25 mW; modulation amplitude, 5 G; temperature, 133 K; and 4 scans averaged. Microwave frequencies were measured with an EIP model 331 counter.

RESULTS

Visible Absorption Spectroscopy. Native amicyanin exhibits a major absorbance maximum centered at 595 nm and a minor absorbance maximum at 464 nm (*12*). For pure native amicyanin, the ratio of absorbance at 280 to 595 nm ($\epsilon_{280}/\epsilon_{595}$) is approximately 4. Surprisingly, the $\epsilon_{280}/\epsilon_{595}$ for the as-isolated M98A and M98Q amicyanins were each greater than 10 (Figure 1A and B), despite each appearing pure on the basis of SDS−PAGE. Incubation of the proteins with ferricyanide did not alter this ratio, indicating that the lack of absorbance at 595 nm was not because the protein was in the reduced state. It is known that apoamicyanin, which lacks copper, may be readily converted to amicyanin by stoichiometric addition of Cu^{2+} (*31*). However, the addition of Cu^{2+} to the as-isolated M98A and M98Q amicyanins caused no change in the absorption spectra, indicating that the protein was not lacking absorbance because it was an apoprotein. Treating the as-isolated mutant amicyanins with EDTA followed by the addition of Cu^{2+} also had no effect on the spectra. It was possible to obtain absorption spectra for these mutants more characteristic of type 1 copper proteins by unfolding the M98A and M98Q amicyanins using 6 M guanidine-HCl in the presence of EDTA and DTT and then adding Cu^{2+} to the refolded protein (Figure 1A and B). After this procedure, the $\epsilon_{280}/\epsilon_{595}$ ratios

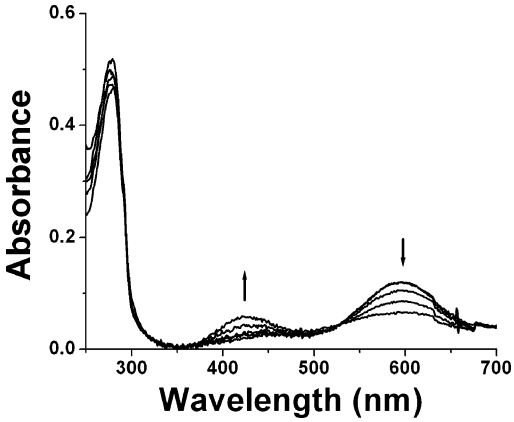

FIGURE 2: pH titration of spectral changes of M98A amicyanin (26 μM) in 50 mM BisTris propane buffer. The arrows indicate the direction of the spectral change as pH increases from 7.0 to 9.0.

for M98A and M98Q amicyanins decreased to approximately 5 and 4, respectively. The exact ratio varied with preparation, which is why approximate values are given. The visible absorption spectra that were obtained for these mutant amicyanins were similar but not identical to that of native amicyanin (Figure 1 C). The minor absorbance maximum at 464 nm also exhibited by native amicyanin shows a ratio of $\epsilon_{595}/\epsilon_{464}$ of 8.9 (*12*). M98Q exhibited a minor absorbance maximum at 464 nm as well; however, it was more intense than that of native amicyanin with a ratio of $\epsilon_{595}/\epsilon_{464}$ of 5.9. The spectrum of the reconstituted M98A amicyanin exhibited a minor absorbance maximum at 464 nm with a ratio of $\epsilon_{595}/\epsilon_{464}$ of 8.0, which is closer to that of native amicyanin than to that of M98Q amicyanin. In addition, M98A amicyanin exhibited some weak, broad absorbance between 300 and 400 nm, which was not consistently seen in each preparation.

The visible absorption spectrum of native amicyanin does not change significantly with pH. In contrast, the absorption spectrum of oxidized M98A amicyanin exhibits a decrease in absorbance at 595 nm as pH is increased from 7.0 to 9.0 (Figure 2). In addition to this change in the major peak, the minor peak centered around 464 nm increases in absorbance and shifts to a lower wavelength. These spectral changes are irreversible. No such pH-dependent spectral changes are seen with M98Q amicyanin.

The visible absorption spectrum of native amicyanin does not change significantly on freezing. In contrast, a change

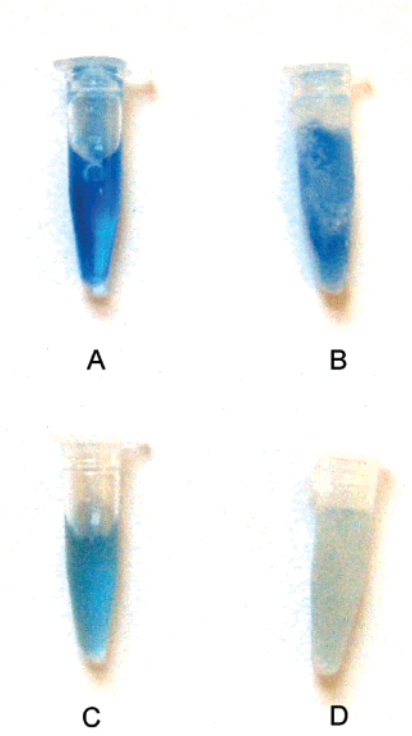

FIGURE 3: Effect of freezing on the color of amicyanin. (A) Solution of native amicyanin; (B) A after freezing; (C) solution M98A amicyanin; (D) C after freezing. Samples were in 10 mM potassium phosphate at pH 7.5 containing 10% ethylene glycol. Samples were frozen by placing them in a −80 °C freezer.

in color of M98A amicyanin was observed when it was frozen. Like native amicyanin, M98A amicyanin appears blue in solution at room temperature; however, upon freezing, the blue color of M98A amicyanin diminishes, and the frozen sample appears gray, whereas native amicyanin remains blue (Figure 3). This color change is reversible, and M98A amicyanin returns to blue after thawing.

Metal Analysis. Wild-type amicyanin contains a single copper per protein molecule. This was confirmed by ICP-OES spectrometry, which yielded a value for native amicyanin of 0.89 Cu per molecule and no evidence of significant presence of any other metals (Table 2). Given the relatively weak ϵ_{595} of M98A and M98Q amicyanins as isolated and the increase in ϵ_{595} after the reconstitution protocol, it was of interest to determine the metal content of these mutant proteins as-isolated and after copper reconstitution. ICP-OES spectrometry indicated that the as-isolated mutant amicyanins each contained <0.1 copper per molecule, consistent with their weak absorbance. The predominant metal that was present instead was zinc. Each mutant amicyanin contained about 0.9 zinc per molecule. The proteins were washed with 1 mM EDTA to remove any surface-bound metal or metal that might be weakly bound to the active site. The zinc content of the as-isolated proteins did not significantly change after the EDTA wash, indicating that it was tightly bound in the metal site. After protein unfolding and zinc removal and copper reconstitution (see Experimental Procedures), each mutant contained <0.1 zinc and >1 copper per molecule. No significant amounts of other metals were detected. After the reconstituted proteins were subsequently washed with EDTA, the copper content decreased to 0.89 per molecule of M98A amicyanin and 0.61 per molecule of M98Q amicyanin. The visible absorption spectra of M98Q and M98A amicyanins before and after washing with EDTA did not show any significant changes. It is not surprising that some nonspecifically bound copper is removed after treatment with EDTA because the proteins are treated with excess copper during the copper reconstitution procedure. It is surprising that the M98Q amicyanin copper content is markedly less than 1 per molecule after EDTA treatment. Because the absorption spectrum of M98A amicyanin does not significantly change after the EDTA treatment, this suggests that no type 1 copper was removed by EDTA. This means either that the reconstitution of M98Q amicyanin resulted in only partial loading of the metal binding site or that some population of the metal binding sites contained copper that was not in the type 1 geometry.

Table 3: Stabilities of Oxidized and Reduced Native, M98A, and M98Q Amicyanins[a]

	T_m values (°C)	
protein	oxidized	reduced
native amicyanin	67.7 ± 0.1 (major) 75.5 ± 0.2 (minor)	62.0 ± 0.1
M98A amicyanin	48.0 ± 0.1	50.3 ± 0.1
M98Q amicyanin	58 ± 0.1 (major) 64.0 ± 0.1 (minor)	52.0 ± 0.1 (major) 63.0 ± 0.1 (minor)

[a] Samples were scanned at a rate of 1 °C/min from 15 to 105 °C in 0.1 M potassium phosphate at pH 7.5.

Thermal Stability. The thermal stabilities of the reconstituted M98A and M98Q amicyanins are greatly reduced relative to that of native amicyanin (Table 3). Solution DSC has been used previously to characterize the thermal stability of amicyanin (*28*). The DSC profile of native, oxidized amicyanin is characterized by two thermal transitions with T_m values of 68 and 76 °C. The first transition corresponds to the temperature-dependent disruption of the copper coordination sphere, whereas the second transition represents the further irreversible unfolding of the protein. At pH 7.5, the DSC profile of reduced amicyanin exhibits a single transition at 62 °C as the temperature dependence of these two processes become indistinguishable. The major transitions for oxidized and reduced M98Q amicyanin each

Table 2: ICP Analysis of Native, M98A, and M98Q Amicyanins

	native amicyanin		M98A amicyanin		M98Q amicyanin	
protein form	Cu	Zn	Cu	Zn	Cu	Zn
			as-isolated			
−EDTA wash	0.894 ± 0.130	<0.003	0.065 ± 0.006	0.92 ± 0.01	0.097 ± 0.019	0.90 ± 0.01
+EDTA wash	0.858 ± 0.170	<0.002	0.065	0.870	0.0660	0.950
			copper-reconstituted			
−EDTA wash			1.77	0.0	1.13 ± 0.14	0.084 ± 0.017
+EDTA wash			0.890	0.015	0.608 ± 0.17	0.052 ± 0.034

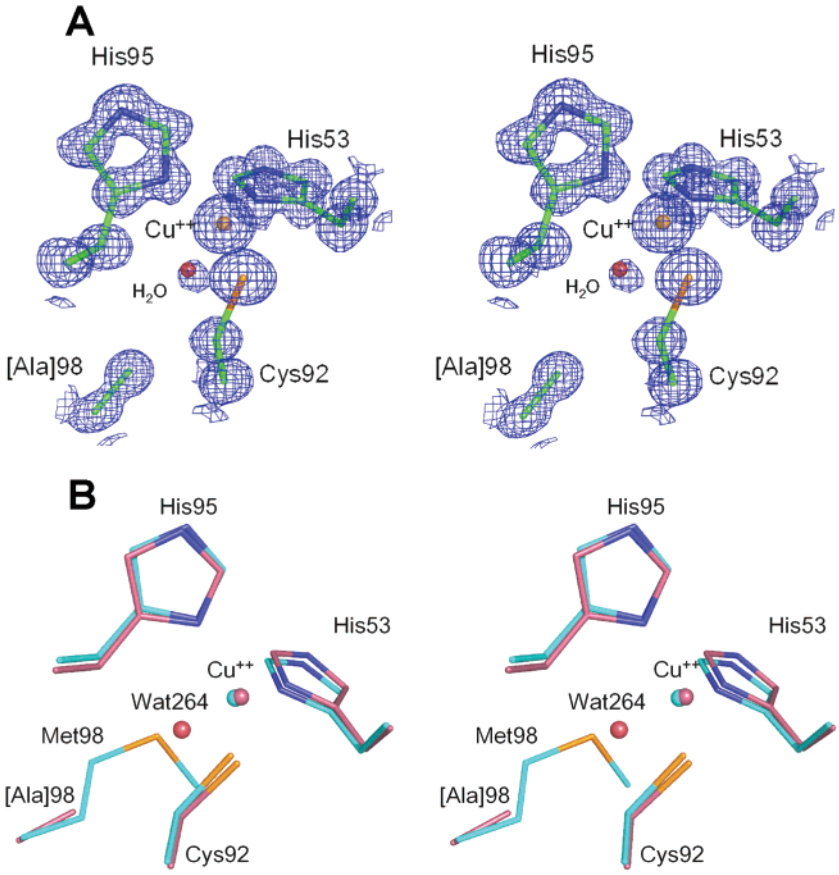

FIGURE 4: Oxidized M98A amicyanin structure. (A) Stereoview of the copper center of oxidized M98A amicyanin with the $2|Fo| - |Fc|$ electron density map contoured at 1.2 σ level. Carbon atoms are green, nitrogen atoms blue, oxygen atoms red, sulfur atoms yellow, and copper atoms brown. (B) Configuration of the copper center of the oxidized form of the M98A mutant of amicyanin (brown) superposed on the 1.30 Å structure of wild-type oxidized amicyanin (cyan). For M98A amicyanin, the carbon and copper atoms are violet and blue, respectively, whereas for the wild type, they are both cyan. For both structures, nitrogen atoms are blue, oxygen atoms are red, and sulfur atoms are brown.

occurred at temperatures about 10 °C lower than those for native amicyanin (Table 3). M98A amicyanin exhibited even lower thermal stability with T_m values of 48 and 50 °C for the oxidized and reduced states, respectively. DSC of the as-isolated Zn-containing M98Q and M98A amicyanins yielded similar profiles each with T_m values approximately 4 °C higher than those of the respective reconstituted Cu-containing proteins (data not shown).

Crystal Structure. The structures of the crystals of oxidized Cu-containing M98A and M98Q amicyanins were refined at atomic resolution (0.90−1.00 Å resolution). An analysis of the structural quality of these crystals using PROCHECK indicates that all of the residues for the four crystals are in either the most favored or the additionally allowed regions of the Ramachandran plot (*32*). For M98A amicyanin, the oxidized crystal contained two residues each in two alternate conformations (Lys38 and Met72), whereas the reduced crystal had four residues (Ser9, Met72, Asp89, and His95). For M98Q amicyanin, the crystals in both oxidation states had only one residue in two alternate conformations (Gln98), and the reduced form also had the copper ion occupying two alternate conformations.

Structure of M98A Amicyanin. The overall conformation of oxidized M98A amicyanin is very similar to that of the wild-type protein, exhibiting 0.20 Å rmsd between equivalent Cα atoms for all 105 residues. However, its copper binding site is different from that of wild-type amicyanin with respect to the identity and position of the axial ligand. The three equatorial ligands are the same, His53, Cys92, and His95, but the fourth ligand, methionine in the wild-type, is replaced by alanine, whose Cβ side chain is 5.5 Å from the copper. However, a water molecule (#264) is located near the site (within ~0.8 Å) of the S$^\gamma$ atom of methionine of the wild-type protein (Figure 4A) and is 2.41 Å from the copper (Table 4), thereby forming the fourth ligand. The copper ion is displaced from its position in the wild-type protein by about 0.3 Å in the direction away from the Met98. The distances from the copper to the three retained ligands are similar to those in wild-type amicyanin (Table 4), and the ligand arrangement is also similar to that of the wild type (Figure 4B). The electron density of Wat264 is considerably weaker than that of other waters (Figure 4A), and the B-value (30.2 Å^2) is considerably higher than those of other internal waters that are typically between 6 and 11 Å^2. However, Wat264 makes no hydrogen bonds to any protein ligand or other water and is poorly stabilized in comparison with other internal waters that usually form hydrogen bonds to two or three other atoms. This probably results from the hydrophobic surroundings normally found for methionine side chains and may be the basis for changes in geometry of the metal site and corresponding spectral changes that are observed at high pH and upon freezing (discussed earlier, Figures 2 and 3).

Table 4: Bond Lengths from the Copper Center of Oxidized and Reduced Native, M98A, and M98Q

	oxidized M98A	reduced M98A	oxidized M98Q	reduced M98Q	native oxidized amicyanin[a]
His95−Cu (Å)	2.005 ± 0.009	3.506 ± 0.127	2.023 ± 0.013	2.062 ± 0.010[b] 2.927 ± 0.084[c]	2.03
Cys92−Cu (Å)	2.141 ± 0.003	1.904 ± 0.013	2.161 ± 0.005	2.220 ± 0.003[b] 2.096 ± 0.009[c]	2.08
His53−Cu (Å)	1.949 ± 0.008	1.738 ± 0.022	1.980 ± 0.010	2.052 ± 0.008[b] 1.784 ± 0.011[c]	1.96
axial ligand −Cu (Å)	2.414 ± 0.104[d]	[e]	2.123 ± 0.028[f] 2.447 ± 0.041[g]	2.087 ± 0.016[b,f] 2.588 ± 0.084[c,g]	2.91
trigonal plane −Cu (Å)[h]	0.14	[e]	0.42	0.55	0.30

[a] 1.30 Å structure (pdb code 1AAC). [b] Distance to the major copper atom. [c] Distance to the minor copper atom. [d] Distance to oxygen from water WAT264. [e] No axial ligand or equatorial plane present. [f] Distance to Gln98 OE2, major conformation. [g] Distance to Gln98 OE2, minor conformation. [h] Distances from the major copper center to the equatorial plane defined by atoms His53 $N^{\delta 1}$, Cys92 SG, and His95 $N^{\delta 1}$.

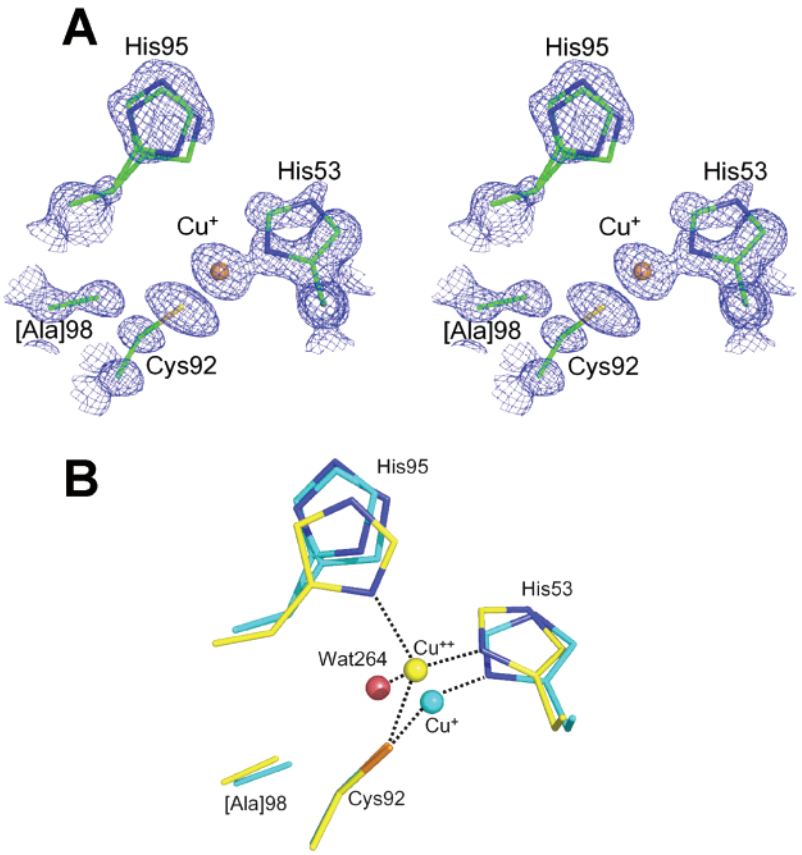

FIGURE 5: Reduced M98A amicyanin structure. (A) Stereoview of the copper center of reduced M98A amicyanin with the $2|Fo| - |Fc|$ electron density map contoured at the 1.0 σ level. The atom coloring scheme is the same as that in Figure 4A. (B) Oxidized M98A amicyanin (carbon and copper, yellow) superposed on reduced M98A amicyanin (carbon and copper, cyan). All nitrogen, oxygen, and sulfur atoms are blue, red, and brown, respectively.

The overall structure of reduced M98A amicyanin is also similar to that of the wild-type protein, except for the segment from residues 17−20, which are known to vary in conformation among various amicyanin structures (*18*), leading to an rmsd of 0.49 Å for 105 Cα atoms. Omission of these four residues results in a rmsd of 0.35 Å. However, when compared to the oxidized M98A amicyanin structure, a dramatic change is seen in the coordination of the copper ion (Figure 5A). Only His53 and Cys92 remain bound to the copper (Table 4). The copper moves by about 1 Å in a direction away from His95, which itself moves away from the copper to a distance of about 3.5 Å from the side chain (Figure 5B). No water molecules are seen in the vicinity of the copper ion to provide additional coordination. The electron density for the copper ion is also very weak and was refined to about 40% occupancy, suggesting that some loss of copper had occurred upon reduction of the crystal. The water structure around His95 also indicates that this side chain has two alternate conformations.

Structure of M98Q Amicyanin. The overall structures of both oxidized and reduced M98Q amicyanins show differences from that of the oxidized wild-type amicyanin, similar to those discussed for reduced M98A amicyanin. The largest differences (1−2 Å in Cα position) are localized to the variable 17−20 segments and drop to a rmsd of 0.32 and 0.25 Å, respectively, when this segment is omitted. However,

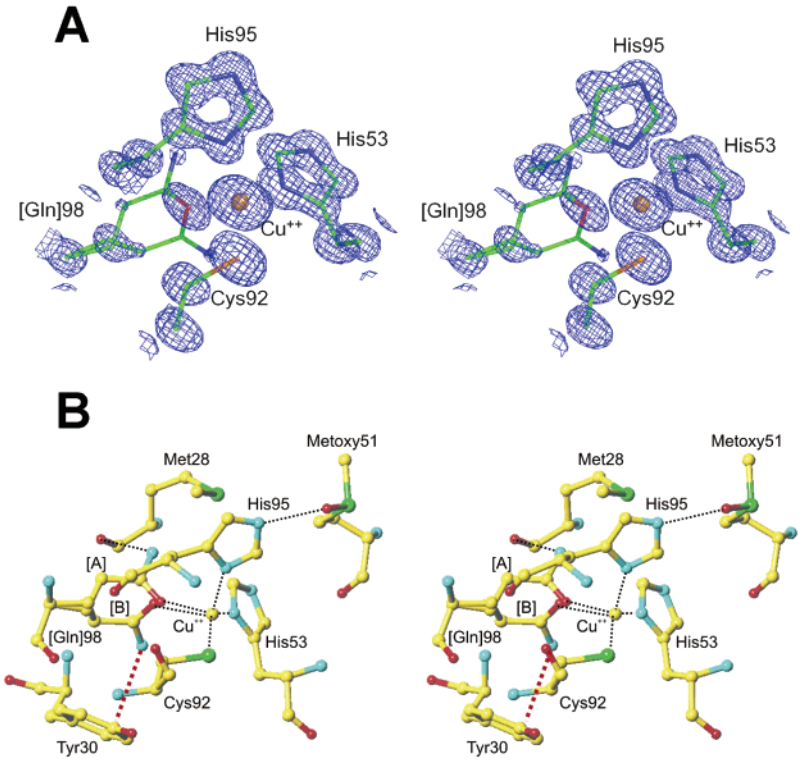

FIGURE 6: Oxidized M98Q amicyanin structure. (A) Copper center of oxidized M98Q amicyanin with $2|Fo| - |Fc|$ map contoured at the 1.8 σ level. The atom coloring scheme is the same as that in Figure 4A. (B) Configuration of the copper center in the oxidized form of the M98Q mutant of amicyanin. The two alternate conformers of Gln98 are shown as [A], the major one (54%), with $N^{\epsilon 2}$ hydrogen bonded to Met28 O and [B], the minor one (46%), with $N^{\epsilon 2}$ located 3.6 Å above the plane of Tyr30. The atom coloring scheme is as follows: carbon, yellow; nitrogen, cyan; oxygen, red; and sulfur, green. Coordination and hydrogen bonds are shown as black dashed lines, and the Gln98−Tyr30 interaction is shown as a thick red dashed line.

in contrast to what was seen with M98A amicyanin, the oxidized and reduced M98Q amicyanin structures are closer to each other, differing by a rmsd of 0.19 Å for all Cα atoms.

The copper coordination in the oxidized M98Q amicyanin structure is the same as that in wild-type amicyanin except that the axial ligand, Met98, is now replaced by Gln98 (Figure 6A). Gln98 exists in two conformations. In the major conformer (54% occupancy), Gln98 is oriented so that OE1 is coordinated to the copper ion (2.12 Å), and $N^{\epsilon 2}$ donates a hydrogen bond to the carbonyl oxygen of Met28 (2.68 Å) (Figure 6B, Table 4). In the minor conformation (46% occupancy), where Gln98 differs by approximately 90° by rotation about its Cα−Cβ bond, one side chain atom (most likely OE1) is coordinated to the copper ion (2.45 Å, Table 4), whereas the other atom ($N^{\epsilon 2}$) projects into the protein interior but forms no hydrogen bonds. It is, however, located above the ring of tyrosine 30 at a minimal distance of 3.5 Å from the plane of the ring (Figure 6B). This situation is analogous to the orientation of Gln99 in stellacyanin, where the $N^{\epsilon 2}$ atom is located 3.3 Å above the plane of Trp13 (*3*). Regardless of the conformation of Gln99, the distances from the copper to the three retained ligands are similar to those in wild-type amicyanin. However, the copper is further removed from the trigonal plane formed by these ligands (Table 4). This is notable given the observed increase in rhombicy of the type 1 copper that is observed in its EPR spectrum (discussed later).

In the reduced M98Q amicyanin structure, the copper ion is disordered, occupying two positions separated by 0.89 Å (Figure 7A). The major copper site (~70% occupancy) corresponds closely in position (0.33 Å) to the copper site in oxidized M98Q amicyanin (Figure 7B). The side chain of Gln98 is also disordered, its two conformations being very similar to those in the oxidized mutant, differing by ~90° by rotation about the Cα−Cβ bond. The conformation in which $N^{\epsilon 2}$ is hydrogen bonded to the carbonyl of Met28 is the major one (also ~70% occupancy). On the basis of the structure, the copper in the major site can be considered to have a more rhombic symmetry, whereas the minor site is more similar to that in the reduced M98A structure, having two strong ligands (His53 and Cys92) and considerably weaker coordination (Table 4 and Figure 7C)

In both the oxidized and reduced crystals of M98Q amicyanin, the sulfur atom of Met51 was found to contain an oxygen atom covalently attached to its S^{γ} atom, thereby forming the sulfoxide form of the side chain. In each case, the oxygen site appears to be fully occupied, and its thermal parameters are similar to those of other well ordered side chains. The oxygen atom is close enough to the $N^{\epsilon 2}$ atom of His95 to form a strong hydrogen bond of 2.68 Å in length in the oxidized structure (Figure 3B) and 2.70 Å in the reduced structure. One other mutant crystal of amicyanin has been reported to contain an oxidized methionine at position 51, that of the P94A mutant (*19*), and oxidized forms of Met51 have been observed occasionally in wild-type amicyanin crystals that have undergone extensive X-ray exposure (unpublished results). To determine whether the oxidation of Met51 had occurred prior to crystallization as a consequence of the mutation or afterward as a consequence of X-ray exposure, the same preparation of M98Q amicyanin that was used for crystallography was subjected to analysis by mass spectrometry. The results showed that the observed

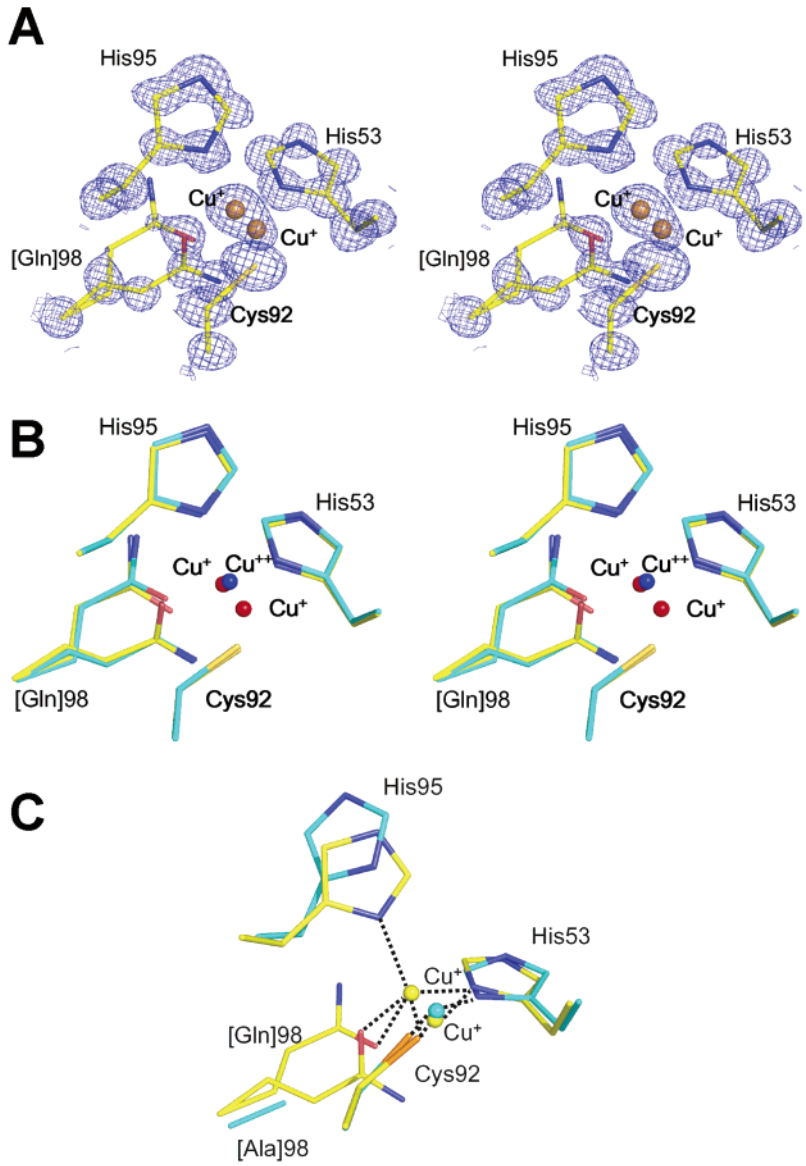

FIGURE 7: Reduced M98Q amicyanin structure. (A) Copper center of oxidized M98Q amicyanin with $2|Fo| - |Fc|$ map contoured at the 1.0 σ level. The atom coloring scheme is the same as that in Figure 4A. (B) Skeletal diagram of reduced M98Q amicyanin (yellow carbons) superposed on oxidized M98Q amicyanin (cyan carbons). The two reduced copper atoms are red, and the oxidized copper is blue. All remaining nitrogen, oxygen, and sulfur atoms are blue, red, and gold, respectively. (C) Skeletal diagram of reduced M98Q amicyanin (yellow carbons and copper) superposed on reduced M98A amicyanin (cyan carbons and copper). The colors of the remaining atoms are the same as those in Figure 4B.

molecular mass is that expected for M98Q amicyanin with no modified methionine residues or any indication of modifications of other amino acids (data not shown). Therefore, the presence of oxidized Met51 in the M98Q amicyanin structures appears to be an artifact of the crystallographic investigation and should have no effect on the solution properties of the mutant.

Electron Paramagnetic Resonance Spectroscopy. The X-band EPR spectra of M98A and M98Q amicyanins were clearly different from that of native amicyanin (Figure 8). The X-band EPR spectra of the native amicyanin shows a single type 1 copper signal with nearly axial symmetry characterized by four hyperfine lines centered at $g_{||} = 2.24$ separated by $A_{||} = 53$ G (Table 5 and Figure 8). After native amicyanin was washed with EDTA, the spectrum was unchanged, except for a little better resolution of the copper hyperfine lines in the $g_{||}$ region. Q-band and S-band EPR spectra were also acquired for each protein (Figure 9).

M98Q Amicyanin. The X-band spectrum of reconstituted M98Q amicyanin exhibited both type 1 and type 2 copper signals (Figure 8A). The type 2 signal ($g_{||} = 2.32$, $A_{||} = 150$ G) was lost after the EDTA wash, which removes weakly bound copper following the reconstitution procedure, leaving a type 1 copper signal with $g_{||} = 2.27$ (Figure 8B). Naturally occurring Cu consists of a mixture of 69.2% ^{63}Cu and 30.8% ^{65}Cu. To obtain a better resolution of the copper hyperfine lines in the high field region, M98Q amicyanin was prepared, which contained only ^{63}Cu. The X-band EPR spectrum of ^{63}Cu M98Q amicyanin (Figure 10) allowed the assignment of $A_x = 64$ G and the high field line in the $g\perp$ region is assigned to g_x=2.04. The middle of the three lines in the $g\perp$ region ($g\perp = 2.09$) may be due to some residual type 2 copper as well as type 1 copper. After washing with EDTA, the ratio of the total peak-to-peak height in the $g\perp$ region divided by the peak-to-peak height for the middle line increased to 2.5 from 1.7.

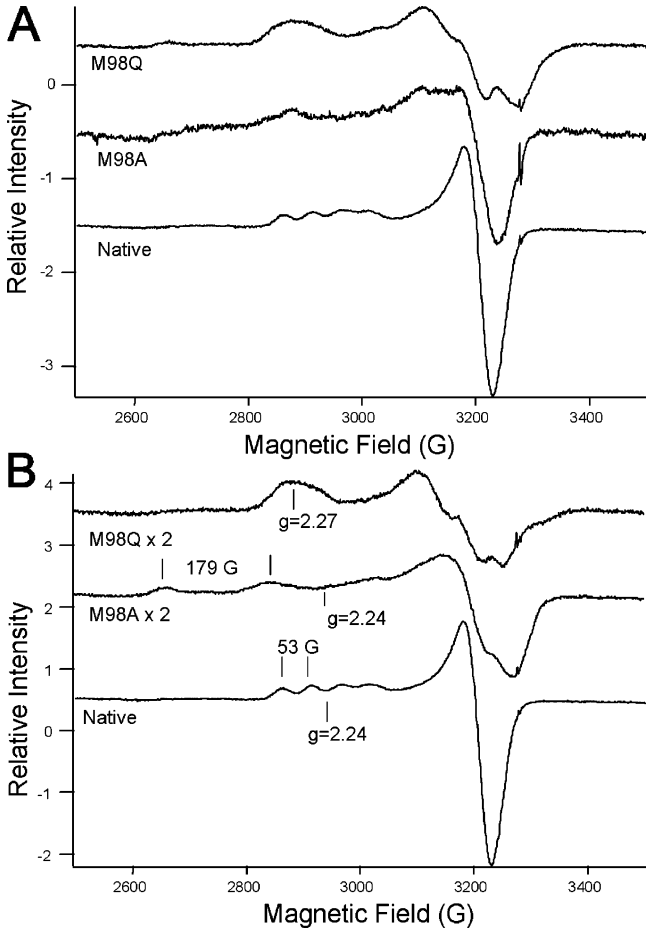

FIGURE 8: X-band EPR spectrum of oxidized native amicyanin (200 μM), reconstituted M98A amicyanin (200 μM), and reconstituted M98Q amicyanin (200 μM) in 10 mM potassium phosphate at pH 7.4 containing 5% glycerol. The spectra of the proteins were recorded before (A) and after (B) washing the samples in buffer containing EDTA.

Table 5: X-band EPR Parameters of Native, M98A, and M98Q Amicyanins

	type 1 signal		type 2 signal	
amicyanin	g	A (G)	g	A (G)
native	**2.24**	**53**		
M98A[a]	2.31		**2.24**	**179**
M98Q[b]	**2.27**	**23**[c]	2.32	150
stellacyanin[d]	2.28	34		

[a] Type 1 signal is a minor component not observed in all preparations. [b] Type 2 signal is a minor component, which is lost after the EDTA wash. [c] Estimated value from line width (Figure 10). [d] Taken from ref 33.

The Q-band EPR spectrum of M98Q amicyanin (Figure 9A) shows an increase in the separation of g_x and g_y and also broadening due to the strain of g_x and g_y. The three g-values (Table 6) indicate a change from the nearly axial type 1 copper configuration to a more rhombic configuration upon switching Met to Gln. This is consistent with the crystal structure of oxidized M98Q amicyanin, which exhibited an increase in distance from Cu^{2+} to the trigonal plane defined by the three equatorial ligands (Table 4). The g_z line (2.27) in the Q-band spectrum and broad peaks in the $g\perp$ region were observed (Table 6 and Figure 9A). Q-band EPR spectra of ^{63}Cu M98Q yields a higher resolution of hyperfine lines (Figure 10) and confirms the values of g_z, g_x, and g_y (Table 6). The EPR parameters reported for stellacyanin are $g_z = 2.282$, $g_y = 2.075$, $g_x = 2.018$ (Table 6), and $A_x^{Cu} = 60$ G (*33*), which are similar to those of M98Q. Even though the signals from the S-band EPR spectrum of M98Q amicyanin (Figure 9B) overlap more than those at the X-band, the S-band spectrum is consistent with the g-values determined at the X-band. Even at the S-band, the copper hyperfine lines for M98Q were not resolved in the $g_{||}$ region, which may be attributed to the presence of more than one type 1 copper signal. This is consistent with the observation of two conformers of Gln98 in the crystal structure of oxidized M98Q amicyanin (Figure 6).

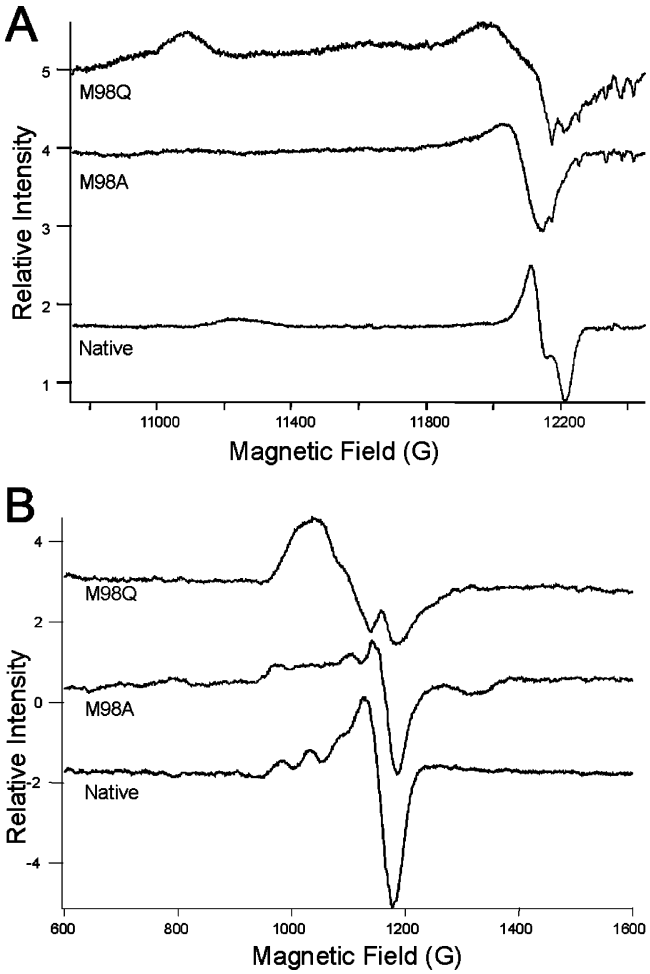

FIGURE 9: Q-band (A) and S-band (B) EPR spectra of oxidized native amicyanin (200 μM), M98A amicyanin (200 μM), and M98Q amicyanin (200 μM) in 10 mM potassium phosphate at pH 7.4 containing 5% glycerol.

M98A Amicyanin. X-band EPR spectra of M98A consistently showed a type 2 copper signal before and after EDTA washing with $g_{||} = 2.24$ and $A_{||} = 179$ G (Table 5, Figure 8). In particular, the large $A_{||}$ value compared to that of a normal type 1 copper center clearly indicates the presence of primarily a type 2 copper site. In one of the samples examined, it was also possible to observe a minor signal attributed to a type 1 copper signal (Table 5). At higher microwave frequency, 35 GHz, in the Q-band EPR spectrum, $g\perp$ was observed but not resolved into g_y and g_x (Figure 9A), nor were these signals resolved in ^{63}Cu M98A amicyanin. The $g_{||}$ region was not detected because the intensity of the lines was too weak. This is typical for a square planar

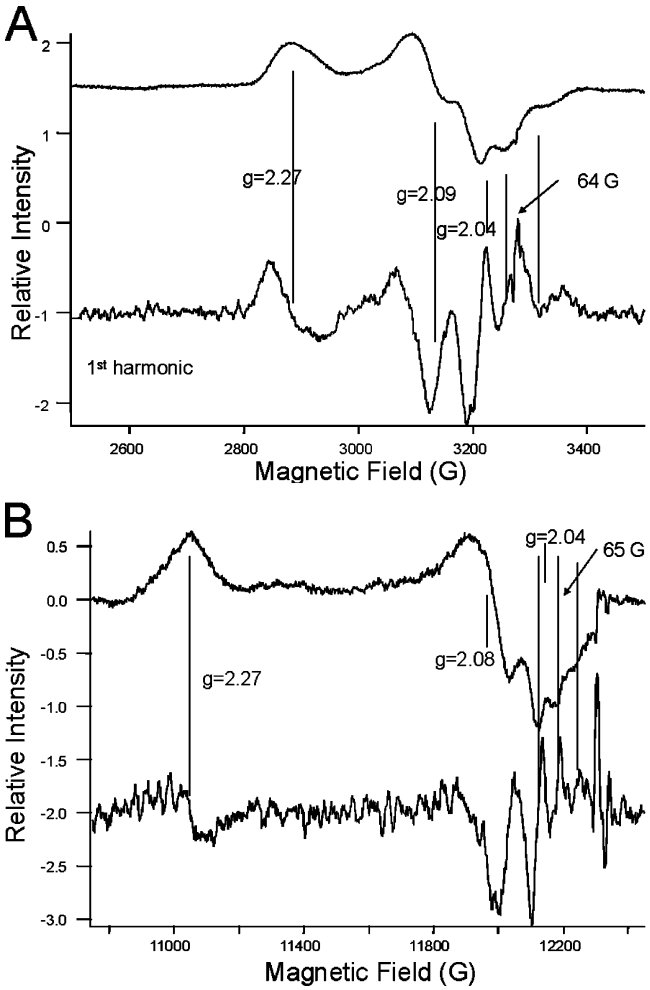

FIGURE 10: X-band (A) and Q-band (B) EPR spectra of ^{63}Cu M98Q amicyanin (270 μM) in 10 mM potassium phosphate at pH 7.4 containing 5% glycerol. The values for g_z, g_y, and g_x and the hyperfine splittings for A_x^{Cu} are marked in both the X-band and Q-band spectra to show the precision of the values from the two frequencies. The spike on the high field side of the Q-band spectra is due to a background signal.

configuration under these conditions. At a lower 3.36 GHz (S-band) frequency, $g_{||}$, $A_{||}$, and $g\perp$ could be obtained but no nitrogen superhyperfine was resolved (Figure 9B). The EPR results that describe M98A amicyanin as having primarily a type 2 copper are in apparent conflict with the crystal structure and visible absorption spectra, which are characteristic of a type 1 copper site. This apparent discrepancy may be explained by a temperature-dependent change in the copper center, as indicated by the observation that oxidized M98A amicyanin exhibits a change in color on freezing (Figure 3 and discussed later).

DISCUSSION

Metal Specificity and Protein Stability. ICP-OES spectrometry indicated that the as-isolated M98A and M98Q amicyanins contain tightly bound zinc rather than copper. After unfolding of the protein, the removal of zinc, and incubation with Cu^{2+}, copper-containing mutant proteins could be generated and studied. Recombinant type 1 copper proteins are sometimes isolated with zinc bound rather than copper when they are expressed in the cytoplasm of *E. coli*. That is because there is virtually no free copper in the cytoplasm. However, our recombinant amicyanin is expressed in the periplasm (*21*), and the growth medium is supplemented with 120 μM $CuSO_4$. No evidence for zinc-bound amicyanin has ever been observed during the expression of recombinant wild-type or several other mutant amicyanins, which we have previously expressed and characterized. Thus, the M98A and M98Q mutations have significantly increased the preference for the incorporation of zinc relative to copper during the assembly of the protein in vivo. When the axial methionine ligand of two other type 1 copper proteins was mutated to glutamine, M121Q azurin (*34*) and M92Q plastocyanin (*8*), each also showed an increased affinity for zinc after initial isolation.

Table 6: Q-band EPR Parameters of M98Q Amicyanin, ^{63}Cu M98Q Amicyanin, and Stellacyanin

	g_x	g_y	g_z	A_x (G)
M98Q	2.04	2.08	2.26	poorly resolved
^{63}Cu M98Q	2.04	2.08	2.27	65
stellacyanin[a]	2.02	2.08	2.28	60

[a] Taken from ref 33.

For amicyanin, the identity of the distal axial ligand plays a significant role in determining the metal specificity of the metal binding site. On the basis of the similar observations with the azurin and plastocyanin mutants (*8*, *34*), this appears to be a general feature of type 1 copper proteins. An exception to this rule, however, is stellacyanin, which is atypical of type 1 copper proteins in that the native protein uses a glutamine residue rather than a methionine to provide the axial ligand. Even so, stellacyanin binds copper and not zinc. Because there is no significant difference in the ionic radii (73 pm for Cu^{+2} and 74 pm for Zn^{+2}) (*34*) and charge between the zinc and copper, it is not clear what accounts for the discrimination. According to the rack-induced bonding concept (*35*), the bound metal ion in cupredoxins is forced to adopt a coordination geometry determined by a rigid peptide conformation. The data for the Met98 amicyanin mutants suggest that the ligand geometry of the active site can accommodate a range of metals and that the identity of the axial ligand is a significant determinant of the metal that is to be incorporated. In the case of stellacyanin, the rack-induced folding may be more rigid such that it contributes more to metal specificity than the axial ligand.

The observation that M98A and M98Q amicyanins have a reduced affinity for copper relative to native amicyanin is consistent with the observation that the copper-containing forms of these mutant amicyanins also exhibit significantly lower thermal stability than native amicyanin. We have previously shown (*28*) that two thermal transitions are observed in the DSC profile of oxidized native amicyanin that are initially associated with the disruption of the copper site, followed by the subsequent denaturation of the overall protein. That is why for native amicyanin, the apoprotein that already lacks copper exhibits a single thermal transition at 52 °C (*28*), which is much lower than that of oxidized amicyanin and similar to the values obtained for M98A and M98Q amicyanins. Because the copper center is the focus for the initiation of the temperature-dependent unfolding of amicyanin, the weaker affinity for the copper of M98A and M98Q amicyanins, relative to that of native amicyanin,

facilitates the loss of copper at lower temperature, and this is reflected in decreased thermal stability (Table 3).

Effects of the Introduction of Glutamine as an Axial Copper Ligand in M98Q Amicyanin. For M98Q amicyanin, the increase in absorbance at 464 nm relative to 595 nm (Figure 1) is indicative of a more rhombic site (*10*). This is supported by the crystal structures that show that the coordination of the copper by the amide O of Gln98 moves the copper away from the equatorial plane defined by the other three ligands (Table 4). A similar change is suggested by the altered absorption spectra of M121Q azurin (*34*) and M92Q plastocyanin (*8*). The increased rhombicity is still consistent with a type 1 coordination, although the change in geometry causes an increase in the splitting and broadening of g_x and g_y, which is observed in the EPR spectra. For M98Q amicyanin, the appearance of three *g*-values at 2.27, 2.08, and 2.04 indicates a change from the normal more axial type 1 copper configuration to a more rhombic configuration upon the replacement of Met with Gln (Table 6).

In the Q-band spectrum, the g_z line (2.27 ± 0.01) and broad peaks in the $g\perp$ region were observed (Figures 9A and 10B). The middle, sharper line in Figure 9A is attributed in part to $g\perp$ from a residual small population of M98Q amicyanin that possesses type 2 copper (discussed earlier). The broad lines at $g_y = 2.08$ and $g_x = 2.04$ are attributed to the configuration with a rhombic distortion. The lines are broad due to an increase in strain for M98Q amicyanin relative to that for native amicyanin. The poorly resolved copper hyperfine lines in g_z and g_y may be attributed to a second rhombic geometry that likely arises from the second, less populated conformation of Gln98 as determined from the crystal structure (Figure 6). Even at the S-band, the copper hyperfine lines for M98Q amicyanin in the g_z region were not resolved. Assuming a line shape similar to the line shape for native amicyanin in the $g_{||}$ region, $A_{||}$ for the unresolved copper hyperfine lines from M98Q amicyanin was about 23 G, that is, about half of the value for $A_{||}$ from native amicyanin. To our knowledge, this is the smallest value reported for $A_{||}^{Cu}$ from a type 1 copper site, albeit from a rhombic distorted type 1 site.

The reconstituted M98Q amicyanin also contains a subpopulation of type 2 copper as revealed by the EPR of this sample. However, it is more weakly bound than the type 1 copper as evidenced by its selective removal by the EDTA wash. Type 2 copper centers exhibit square planar geometry with visible absorption spectra that lack distinctive features (*36*) and, therefore, do not contribute to the absorbance maxima centered around 595 nm. This explains why after EDTA treatment the copper content of the reconstituted M98Q amicyanin decreased to 0.61 per molecule, with no concomitant decrease in A_{595}. The fact that the metal binding site of M98Q amicyanin exhibits multiple copper geometries, two type 1 conformers and a weakly bound type 2 copper, indicates that it is not only the identity of the axial ligand that dictates ligation geometry but also its position. The flexibility of the Gln98 side chain in M98Q amicyanin is allowing multiple ligation geometries to exist.

Effects of the Introduction of Water as an Axial Copper Ligand in M98A Amicyanin. The sensitivity of the copper binding site of oxidized M98A amicyanin to pH and temperature likely reflects the fact that a potentially mobile water molecule and not a fixed amino acid residue is providing the axial ligand for Cu^{+2}. The color change observed with M98A amicyanin upon freezing (Figure 3) may be attributed to changes in the lattice matrix upon freezing where the relative flexibility of the ligand environment around Ala98 allows the entry of solvent molecules prior to freezing but locks the solvent molecule into a more sterically immobile lattice that contributes to the alterations in the Cys92$-Cu^{+2}$ charge transfer. Such flexibility that allows the movement of a water molecule within the ligand environment could account for the appearance of type 2 copper signals upon freezing. It is possible that the axial water movement within the matrix upon freezing creates a geometry that appears more square planar than the typical distorted tetrahedral coordination in solution. Clearly, this transition to a type 2 copper site is reversible because M98A amicyanin exhibits a distinct type 1 copper absorbance peak at 595 nm in the aqueous form before freezing and after thawing. The irreversible decrease in the 595 nm peak with a concurrent increase in the 464 nm peak as a function of increasing pH observed in the absorption spectra of M98A amicyanin (Figure 2) suggests that the protein undergoes a pH-dependent transition with a more rhombic appearance and concurrent loss of copper from the active site. It is interesting that the minor peak centered on 464 nm undergoes a shift to a lower wavelength while its magnitude increases with increasing buffer pH. The data suggest that during the process of pH dependent denaturation of M98A, the protein undergoes a conformational change that moves copper away from the equatorial plane, resulting in the appearance of increased rhombicity. In contrast to the effects of freezing, this process is irreversible. The ability to reversibly switch from a type 1 geometry in the aqueous state to a type 2 geometry in the frozen state is a novel observation for a native or mutant cupredoxin. The geometry of the copper in the reduced M98A amicyanin of a nearly linear coordination between only two ligands is also unprecedented for a cupredoxin.

Summary. The replacement of the axial S ligand normally provided by Met with an axial O ligand provided either by Gln or water significantly increased the preference for the incorporation of zinc relative to copper during the assembly of amicyanin in vivo. The replacement of Met98 with Gln yielded a type 1 copper site with increased rhombicity as evidenced by an increase in distance from Cu to the trigonal equatorial plane seen in the crystal structure, the appearance of three *g*-values in its EPR spectrum, and an unusually small $A_{||}^{Cu}$ value for a type 1 copper site. The replacement of Met98 with Ala yielded a type 1 copper site with water providing the axial ligand. The geometry of this site reversibly changed to type 2 on freezing. The crystal structure of reduced M98A amicyanin exhibits an unprecedented ligation geometry in which the His95$-$Cu coordination is broken, and copper is left with only two ligands from His53 and Cys92 in an almost linear coordination. These results indicate that the identity as well as position and rigidity of the axial ligand for the type 1 copper site has a profound influence on its metal specificity, ligation geometry, stability, and spectroscopic properties. It follows that relatively subtle changes in the nature of a metal ligand or its environment, even in the absence of significant overall protein structural changes, may play critical roles in the assembly and properties of metalloproteins in general.

ACKNOWLEDGMENT

We thank the staff at the NE-CAT and the Biocars beamlines of the APS for their assistance and use of equipment. We thank Teresa de la Mora-Rey and Carrie Wilmot at the University of Minnesota for performing mass spectrometry on M98Q amicyanin.

REFERENCES

1. Adman, E. T. (1991) Copper protein structures, *Adv. Protein Chem. 42*, 145−197.
2. Baker, E. N. (1988) Structure of azurin from Alcaligenes denitrificans refinement at 1. 8 Å resolution and comparison of the two crystallographically independent molecules, *J. Mol. Biol. 203*, 1071−1095.
3. Hart, P. J., Nersissian, A. M., Herrmann, R. G., Nalbandyan, R. M., Valentine, J. S., and Eisenberg, D. (1996) A missing link in cupredoxins: crystal structure of cucumber stellacyanin at 1.6 Å resolution, *Protein Sci. 5*, 2175−2183.
4. Piontek, K., Antorini, M., and Choinowski, T. (2002) Crystal structure of a laccase from the fungus Trametes versicolor at 1.90-Å resolution containing a full complement of coppers, *J. Biol. Chem. 277*, 37663−37669.
5. Zaitseva, I., Zaitsev, V., Card, G., Moshkov, K., Bax, B., Ralph, A., and Lindley, P. (1996) The X-ray structure of human serum ceruloplasmin at 3.1 Å: nature of the copper centres, *J. Biol. Inorg. Chem. 1*, 15−23.
6. Cunane, L. M., Chen, Z., Durley, R. C. E., and Mathews, F. S. (1996) X-ray crystal structure of the cupredoxin amicyanin from *Paracoccus denitrificans*, refined at 1.31 Å resolution, *Acta Crystallogr., Sect. D 52*, 676−686.
7. Coremans, J., Poluektov, O. G., Groenen, E. J. J., Warmerdam, G. C. M., Canters, G. W., Nar, H., and Messerschmidt, A. (1996) The azurin mutant Met121Gln: A blue-copper proetin with a strong axial ligand, *J. Phys. Chem. 100*, 19706−19713.
8. Hibino, T., Lee, B. H., and Takabe, T. (1995) Expression and characterization of Met92Gln mutant plastocyanin from *Silene pratensis*, *J. Biochem. 117*, 101−106.
9. Nersissian, A. M., Immoos, C., Hill, M. G., Hart, P. J., Williams, G., Herrmann, R. G., and Valentine, J. S. (1998) Uclacyanins, stellacyanins, and plantacyanins are distinct subfamilies of phytocyanins: plant-specific mononuclear blue copper proteins, *Protein Sci. 7*, 1915−1929.
10. Han, J., Loehr, T. M., Lu, Y., Valentine, J. S., Averill, B. A., and Sanders-Loehr, J. (1993) Resonance Raman excitation profiles indicate multiple Cys-Cu charge transfer transitions in type 1 copper proteins, *J. Am. Chem. Soc. 115*, 4256−4263.
11. Davidson, V. L. (2001) Pyrroloquinoline quinone (PQQ) from methanol dehydrogenase and tryptophan tryptophylquinone (TTQ) from methylamine dehydrogenase, *Adv. Protein Chem. 58*, 95−140.
12. Husain, M., and Davidson, V. L. (1985) An inducible periplasmic blue copper protein from *Paracoccus denitrificans*. Purification, properties, and physiological role, *J. Biol. Chem. 260*, 14626−14629.
13. Husain, M., and Davidson, V. L. (1986) Characterization of two inducible periplasmic c-type cytochromes from *Paracoccus denitrificans*, *J. Biol. Chem. 261*, 8577−8580.
14. Chen, L., Durley, R., Poliks, B. J., Hamada, K., Chen, Z., Mathews, F. S., Davidson, V. L., Satow, Y., Huizinga, E., and Vellieux, F. M. (1992) Crystal structure of an electron-transfer complex between methylamine dehydrogenase and amicyanin, *Biochemistry 31*, 4959−4964.
15. Chen, L., Durley, R. C., Mathews, F. S., and Davidson, V. L. (1994) Structure of an electron transfer complex: methylamine dehydrogenase, amicyanin, and cytochrome c551i, *Science 264*, 86−90.
16. Zhu, Z., Cunane, L. M., Chen, Z., Durley, R. C., Mathews, F. S., and Davidson, V. L. (1998) Molecular basis for interprotein complex-dependent effects on the redox properties of amicyanin, *Biochemistry 37*, 17128−17136.
17. Sun, D., Li, X., Mathews, F. S., and Davidson, V. L. (2005) Site-directed mutagenesis of proline 94 to alanine in amicyanin converts a true electron transfer reaction into one that is kinetically coupled, *Biochemistry 44*, 7200−7206.
18. Ma, J. K., Carrell, C. J., Mathews, F. S., and Davidson, V. L. (2006) Site-directed mutagenesis of proline 52 to glycine in amicyanin converts a true electron transfer reaction into one that is conformationally gated, *Biochemistry 45*, 8284−8293.
19. Carrell, C. J., Sun, D., Jiang, S., Davidson, V. L., and Mathews, F. S. (2004) Structural studies of two mutants of amicyanin from *Paracoccus denitrificans* that stabilize the reduced state of the copper, *Biochemistry 43*, 9372−9380.
20. Davidson, V. L., Jones, L. H., and Zhu, Z. (1998) Site-directed mutagenesis of Phe 97 to Glu in amicyanin alters the electronic coupling for interprotein electron transfer from quinol methylamine dehydrogenase, *Biochemistry 37*, 7371−7377.
21. Davidson, V. L., Jones, L. H., Graichen, M. E., Mathews, F. S., and Hosler, J. P. (1997) Factors which stabilize the methylamine dehydrogenase-amicyanin electron transfer protein complex revealed by site-directed mutagenesis, *Biochemistry 36*, 12733−12738.
22. Chistoserdov, A. Y., Boyd, J., Mathews, F. S., and Lidstrom, M. E. (1992) The genetic organization of the *mau* gene cluster of the facultative autotroph *Paracoccus denitrificans*, *Biochem. Biophys. Res. Commun. 184*, 1181−1189.
23. Diederix, R. E., Canters, G. W., and Dennison, C. (2000) The Met99Gln mutant of amicyanin from *Paracoccus versutus*, *Biochemistry 39*, 9551−9560.
24. Lim, L. W., Mathews, F. S., Husain, M., and Davidson, V. L. (1986) Preliminary X-ray crystallographic study of amicyanin from *Paracoccus denitrificans*, *J. Mol. Biol. 189*, 257−258.
25. Otwinowski, Z., and Minor, W. (1997) Processing of x-ray diffraction data collected by oscillation methods, *Methods Enzymol. 276*, 307−326.
26. Sheldrick, G. M., and Schneider, T. R. (1997) SHELXL: High resolution refinement, *Methods Enzymol. 277*, 319−343.
27. McRee, D. E. (1999) XtalView/Xfit−A versatile program for manipulating atomic coordinates and electron density, *J. Struct. Biol. 125*, 156−165.
28. Ma, J. K., Bishop, G. R., and Davidson, V. L. (2005) Role of the Type I copper center in determining the stability of amicyanin, *Arch. Biochem. Biophys. 444*, 27−33.
29. Froncisz, W., and Hyde, J. S. (1982) The loop-gap resonator: A new microwave lumped circuit ESR sample structure, *J. Magn. Reson. 47*, 515.
30. Hyde, J. S., Newton, M. E., Strangeway, R. A., Camenisch, T. G., and Froncisz, W. (1991) Electron paramagnetic resonance Q-band bridge with GaAS field-effect transistor signal amplifier and low-noise Gunn diode oscillator, *Rev. Sci. Instrum. 62*, 2969−2975.
31. Husain, M., Davidson, V. L., and Smith, A. J. (1986) Properties of *Paracoccus denitrificans* amicyanin, *Biochemistry 25*, 2431−2436.
32. Morris, A. L., MacArthur, M. W., Hutchinson, E. G., and Thornton, J. M. (1992) Stereochemical quality of protein structure coordinates, *Proteins 12*, 345−364.
33. Roberts, J. E., Brown, T. G., Hoffman, B. M., and Peisach, J. (1980) Electron nuclear double resonance spectra of stellacyanin, a blue copper protein, *J. Am. Chem. Soc. 102*, 825−829.
34. Romero, A., Hoitink, C. W., Nar, H., Huber, R., Messerschmidt, A., and Canters, G. W. (1993) X-ray analysis and spectroscopic characterization of M121Q azurin. A copper site model for stellacyanin, *J. Mol. Biol. 229*, 1007−1021.
35. Malmstrom, B. G. (1994) Rack-induced bonding in blue-copper proteins, *Eur. J. Biochem. 223*, 711−718.
36. Dawson, J. H., Dooley, D. M., and Gray, H. B. (1980) Coordination environment and fluoride binding of type 2 copper in the blue copper protein ascorbate oxidase, *Proc. Natl. Acad. Sci. U.S.A. 77*, 5028−5031.
37. Brünger, A. T. (1992) Free R-value: a novel statistical quantity for assessing the accuracy of crystal structures, *Nature 355*, 472−475.

BI0619674